Numerical Investigation on a Rotor Tip-Vortex Instability in Very Low Advance Ratio Flight

Kihoon Chung* and Changjeon Hwang**
Rotor System Department and Rotorcraft Development Division
Korea Aerospace Research Institute, Daejeon, Korea, 305-333

Duckjoo Lee***
Department of Aerospace Engineering,
Korea Advanced Institute of Science of Technology, Daejeon, Korea, 305-701

Jongbong Yim*
KHP Development Center, ADD, Daejeon, Korea, 305-600

Abstract

Helical tip vortex is known as stable vortex structure, however the specific frequency component of far wake perturbation induces the vortex pairing in hover and axial flight. It is expected that the tip vortex pairing phenomena may happen in transition flight and very low advance ratio flight so that inflow may be most nonuniform in the low advance ratio flight. The objectives of this paper are that a tip-vortex instability during the transition from hover into very low advance ratio forward flight is numerically predicted to understand a physics by using a time-marching free-wake method. To achieve the objectives, numerical method is firstly validated in typical axial and forward flights cases. Present scheme with trim routine can predict airloads and inflow distribution of forward flight with good accuracy. Then, the transition flight condition is calculated. The rotor used in this wake calculation is a small-scale AH-1G model. By using a tip-vortex trajectory tracking method, the tip-vortex pairing process are clearly observed in transient flight(μ=0.03) and disappears at a slightly higher advance ratio(μ=0.05). According to the steady flight simulation at μ=0.03, it is confirmed the tip-vortex pairing process is continued in the rear part of rotor disk and not occurs in the front part. Time averaged inflow in this case is predicted as smooth distribution.

Key Word : Rotor Tip Vortex, Vortex Instability, Time Marching Free Wake, Transition Flight, Low Advance Ratio Flight

Introduction

Tip vortices are the most significant aerodynamic feature of a helicopter rotor wake. In contrast to fixed-wing aircraft where the tip vortices trail far downstream, rotor tip-vortices can remain in close proximity to the rotor for a significant amount of time, and are key factors in determining the rotor performance, local blade loads and noise level. However, the fluid mechanics of the rotor wake behavior has not been fully predicted by numerical methods, yet.

* Senior Researcher
** Senior Researcher, Corresponding Author
E-mail: chwang@kari.re.kr, TEL : 042-860-2363, FAX : 042-860-2604
*** Professor

The wakes are genuinely unsteady, which have been observed in various experiments[1, 2]. The unsteady wake motion is becoming a crucial issue in the point of unsteady aerodynamics and aeroacoustics for a certain flight condition in recent years. Landgrebe[1] and Tangler et al.[2] first observed that the tip vortices shed from a two-bladed rotor could interact with each other significantly. Widnall[3] and Gupta & Loewy[4] tried to analyze this pairing phenomenon using linear stability theory. Recent experiments[5, 6] showed more detailed pairing process of two different tip-vortices. The tip-vortex pairing phenomena of model AH-1G rotor are numerically predicted by using a time marching free wake method and the calculated results are compared with experimental wake pairing visualization data[6]. Quite good agreements could be found in Refs. 7 and 8.

Generally, most of inflow models is not valid in the low advance ratio flight ($\mu < 0.1$) because lots of wake components just beneath the rotor disk make an inflow the most non-uniform[9]. In addition, it is expected that the tip vortex pairing phenomena may happen in transition flight and very low advance ratio flight like an axial flight. The objectives of this paper are that a tip-vortex instability during the transition from hover into very low advance ratio forward flight is numerically predicted to understand a physics by using a time-marching free-wake method[10, 11]. To achieve the objectives, numerical method is firstly validated in typical axial and forward flights cases. Then, the transition flight and very low advance ratio flight condition are calculated. The rotor used in this wake calculation is a sub-scale AH-1G model with a 41-inch radius rotating at 1,800 rpm. This rotor is the same one as used in the experiments of Caradonna et al.[6]. The tip-vortex pairing process is quantified and understood by using a tip-vortex trajectory tracking method.

Tip-Vortex Instability In Axial Flights

Fig. 1 shows a sequence of images of the tip vortex development at a rotor collective angle of 9^{o} and climb rate of 3.5 fps[6]. The tip vortices trailed from two different blades are identified by their index numbers, i.e. an odd numbered vortices are trailed from the same blade and even numbered from the other. The time spacing between each successive frame is not constant, but it was chosen to show the progress of the pairing phenomena. The first frame shows two clear

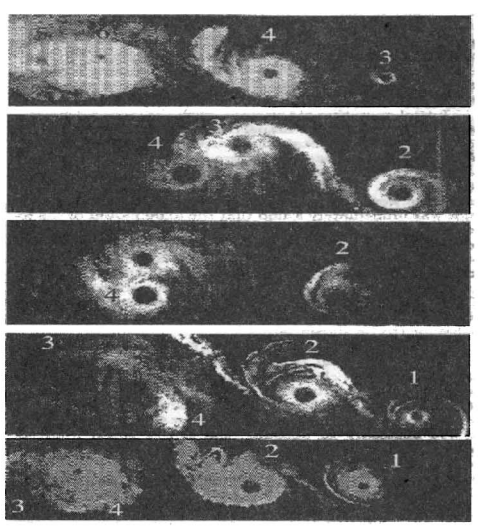

Fig. 1. Sequence of tip-vortex pairing from the individual blade, 9^{o} collective, 3.5 fps climb rate (Ref. 6)

vortices, indexed '3' and '4'. In the next frame, vortex '3' has begun to roll up with '4'. This process continues in the next two frames, until '3' and '4' have essentially interchanged their positions while moving downstream (left direction in Fig. 1).

The notable aspect of this visualization is that the vortex trajectories do not appear to follow a path whose contraction increases monotonically with time. Beyond a certain age, the vortex trajectory tends to expand radially(downward direction in Fig. 1). Moreover, the spacing between the tip vortices seems to change. Such vortex expansion have been noted in many previous tests and visualizations and frequently attributed to being some manifestation of an unstable process. However, the vortex expansion was seen to be a result of adjacent tip vortices beginning to pair together and spiral about each other[6].

Time-marching Free-wake Method

The fluid surrounding the body is assumed to be inviscid, irrotational, and incompressible over the entire flow field, excluding the body's solid boundaries and its wakes. Therefore, a velocity potential $\Phi(\vec{x},t)$ can be defined and the continuity equation in the inertial frame becomes:

$$\nabla^2\Phi = 0 \tag{1}$$

The boundary condition requiring zero normal velocity across the body's solid boundaries is:

$$(\nabla\Phi + \vec{V}_{wake} - \vec{V}) \cdot \vec{n} = 0 \tag{2}$$

Where $\vec{V}_{wake}(\vec{x},t)$ is the induced velocity due to the vorticity field in the wake, $\vec{V}(\vec{x},t)$ is the body surface's velocity, and $\vec{n}(\vec{x},t)$ is the vector normal to the moving surface, as viewed from the blade. Using Green's second identity, the general solution of Eq. (1) can be constructed by integrating the contribution of the basic solution of source (σ) and doublet (μ) distributions over the body's surface:

$$\Phi(\vec{x},t) = \frac{1}{4\pi}\int_{body+wake} \mu\vec{n} \cdot \nabla(\frac{1}{r})ds - \frac{1}{4\pi}\int_{body} \sigma(\frac{1}{r})ds \tag{3}$$

Inserting Eq. (3) into Eq. (2) becomes:

$$\left\{\frac{1}{4\pi}\int_{body+wake} \mu\nabla[\frac{\partial}{\partial n}(\frac{1}{r})]ds - \frac{1}{4\pi}\int_{body} \sigma(\frac{1}{r})ds - \vec{V}\right\} \cdot \vec{n} = 0 \tag{4}$$

The source term is neglected in the case of the thin blade. Thus, only the first part of Eq. (3) is used to represent the lifting surface. The constant-strength doublet panel is equivalent to a closed vortex lattice with the same strength of circulation, ($\Gamma = \mu$). Then the induced velocity of the vortex lattice in Eq. (4), representing the blade, can be obtained by using Biot-Savart's law:

$$\vec{V} = -\frac{1}{4\pi}\int_c \frac{\vec{r}\times\Gamma d\vec{l}}{|\vec{r}|^3} \tag{5}$$

The collocation point is located at the mid-span and three-quarter chord of each panel. The boundary condition of no-flow penetration is satisfied at the collocation point of each lattice. The application of the flow tangency condition(Eq. 4) to the vortex lattice distribution yields the following linear matrix equation that is to be solved:

$$A_{ij}\Gamma_j = R_i \qquad (i,j=1,n) \tag{6}$$

where A_{ij} is the coefficient matrix of normal induced velocity on the i-th element of the blade due to the j-th vortex lattice with the unit circulation, and Γ_j is the unknown circulation value of the blade vortex lattice. R_i is the normal induced velocity at each control point due to the free stream velocity, the blade-moving velocity, and the wake-induced velocity.

A three-dimensional wing trails the bound circulation(Γ) into the wake. Radial variation of bound circulation produces trailed vorticity in the wake, which is parallel to the local free stream direction at each instant when it leaves the blade. Azimuthal variation of bound circulation produces shed vorticity, oriented radially in the wake. The strengths of the trailed and shed vorticity are determined by the radial and azimuthal derivatives of bound circulation at the time the wake element leaves the blade. The bound circulation has a peak near the tip, and quickly drops to zero. The trailed sheet therefore has a high strength(proportional to the radial derivative of Γ) at the outer wake, and quickly rolls up into a concentrated tip vortex. The strength of the trailed shed wake vortex at this time step is set equal to the one of the vortex lattice elements, which is located at the trailing edge of the blade($\Gamma_{T.E.,t} = \Gamma_{wake,t}$). This condition is forced to satisfy the Kutta condition($\gamma_{T.E.} = 0$).

Since the wake surface is force-free, each vortex wake element moves with the local stream velocity, which is induced by the other wake element and the blade. The convection velocity of the wake is calculated in the inertial frame. The vortex wakes are generated at each time step. Therefore, the number of wake-elements increases as the blade is rotating. It is clear that a large number of line elements for the highly curved and distorted wake region like the tip vortex are necessary to describe the vortex filament distortions accurately. In general, computational time for the calculation of the wake distortion is proportional to the square of the vortex element number. Therefore, a curved element is used to reduce the number of elements.

There are many mathematical expressions to represent the three dimensional curves. Generally, cubic spline curves are used to describe the curves. However, the cubic spline curves have certain disadvantages; the cubic spline curves require a large tri-diagonal matrix inversion, and the numerical disturbance of position in any one segment affects all the global curve segments. Therefore, the curve is not adequate to represent the vortex filament motion in strong interaction problems. The parabolic blending curves, employed here, maintain the continuity of the first derivative in space, which is critical to self-induced vortex interactions and interactions with wake and blade. The parabolic blending curve, $C(\xi)$, is given by

$$C(\xi) = (1-\xi)p(r) + \xi q(s) \tag{7}$$

The function of p(r) and q(s) are parametric parabolas through P_1, P_2, P_3 and P_2, P_3, P_4 as shown in Fig. 2, respectively.

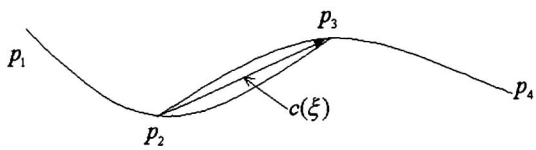

Fig. 2. Parabolic blending method

A generalized parametric blending curve is developed from the assumption of normalized chord length approximation for the position parameters, r and s at P_2 and P_3 which are linearly related with the parameter ξ respectively, i.e. $0 \le r, s, \xi \le 1$. Then, this blending curve is applied to Eq. (5). The induced velocity by a vortex filament with circulation Γ is given by the usual cut-off approach, which is formulated by Moore-Rosenhead[12, 13]. It is defined as

$$\vec{V}=\frac{1}{4\pi}\int_{c}\frac{\vec{r}}{(|\vec{v}|^2+\mu^2)^{3/2}}\times\Gamma\frac{\partial y(\xi,t)}{\partial\xi}d\xi \tag{8}$$

Here, $y(\xi,t)$ is the position vector of a material point denoted by Lagrangian variable ξ at an instance, which describes a vortex filament with circulation Γ. The Rosenhead cut-off parameter μ is used to remove the singularity problem in the Biot-Savart's law at the region very closed to the vortex filaments. In this study, inboard shedding vortex elements as well as the trailed elements are kept for more rigorous representation of vortex dynamics and unsteadiness.

Validation of tip-vortex instability at vertical flight

The rotor used in this wake calculation is AH-1G's 41-inch radius model rotating at 1,800 rpm. The blade is modeled using 5 chordwise panels and 10 spanwise panels. This rotor is the same as that used in the experiments of Caradonna et al.[6]. Twenty-four time-steps are taken per blade revolution and the vortex core radius is taken as 10% of the chord length that is commonly used in rotor wake simulation. The tip-vortex pairing process is quantified by using the trajectory tracking method.

Tip-vortex pairing mechanism

The trajectories of the tip-vortices, which are calculated by using a time-marching free-wake method, are shown in Fig. 3. The left figure shows the three-dimensional view of tip vortex trajectories and the right one shows the cross section view of those.

Fig. 4 shows the tip-vortex roll-up process for collective angle of 11^o at a climb rate of 9.6 fps. In this figure, vortex '3' begins to pair with '4'. This process continues until '3' and '4' interchange their positions while moving downstream. Tip-vortex pairing consists of a turn of the tip-vortex

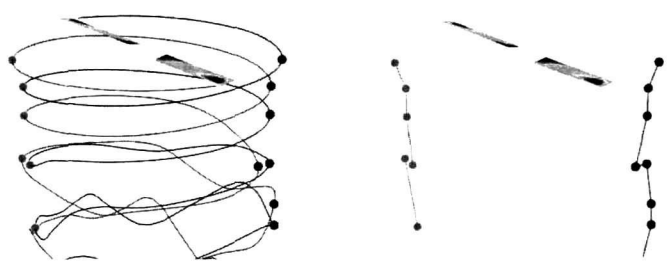

(a) 3D overall view (b) Cross section view

Fig. 3. 3-D view and cross section view of wake geometries at 11^o collective angle, 9.6 fps climb rate

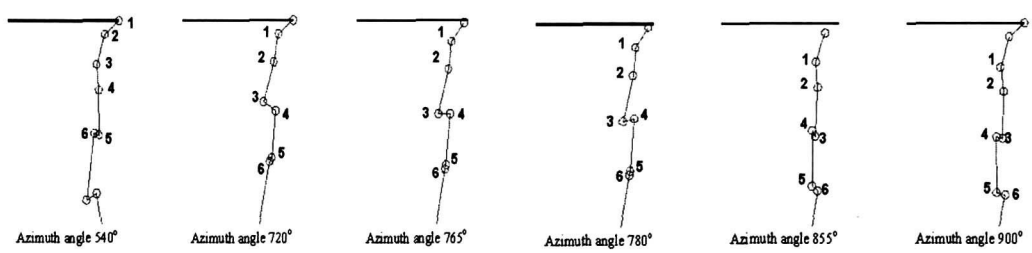

Fig. 4. Tip-vortex pairing process at 11^o collective angle, 9.6 fps climb rate

from one blade rolling around the tip-vortex from the other blade as shown in Fig. 1 even though different conditions.

Comparison with experimental data

Fig. 5 shows the tip-vortices trajectories for collective angle of 11^o at the climb rate of 9.6 fps. These trajectories clearly show that the local radial expansion is the result of adjacent tip vortices beginning to pair together and spiral about each other. The computed wake geometries show excellent agreements with the experimental data as the wake age angle increases after the tip vortices are fully rolled up[8].

Repeatability and instability of tip-vortex pairing

Fig. 6 shows detailed view of tip-vortices geometries generated by two blades during 35 revolutions for collective angle of 11^o with 3.5 fps climb rate. It appears that the initial vortices merge together into a bundle of starting vortex at the beginning of the solution process and that this starting vortex convects away from the rotor at a speed (inverse of the slope in Fig. 6) slower than the individual vortex convection rate and becomes increasingly chaotic with time. Thus the initial wakes in downstream ultimately become unstable, unsteady or chaotic at a sufficient distance from the rotor (z/R>2). In Fig. 6, however, the rotor paths are repeatable form revolution to revolution after about the 20th revolution (7,200 degree azimuth angle) and from the rotor plane up to about the point of vortex pairing. Dashed line in Fig. 6 indicates the approximate boundary of repeatability. Beyond this boundary, the wake is no longer stable or repeatable.

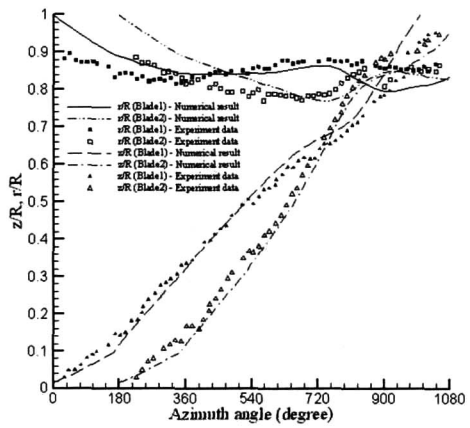

Fig. 5. Wake geometries at 11^o collective angle, 9.6fps climb rate

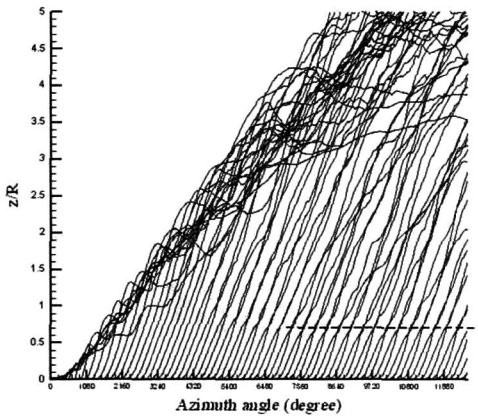

Fig. 6. Detailed tip vortex geometry during 35 revolutions at 11^o collective angle, 3.5 fps climb rate

Validation of Numerical Scheme in Forward Flights

Prediction of airloads in forward flight

To validate the numerical scheme in forward flight condition, the forward flight of two-bladed teetering rotor of AH-1G is simulated. The blade has a rectangular planform with a symmetric airfoil. The aspect ratio of the blade is 9.8 and the linear twist rate is -10^o from root to tip. The calculated flight condition at which the flight test data is available corresponds to an advance ratio of 0.19, tip Mach number of 0.65, and a time-averaged total thrust coefficient of

0.00464[15]. This particular flight condition has also studied by Ahmad et al.[16] and Yang et al. [17].

In the present prediction, the collective pitch is adjusted to match the measured overall thrust. To eliminate the rolling and pitching moment, the lateral and longitudinal cyclic pitch angles were also trimmed automatically. The trimmed first blade harmonics (in degrees) are given in Table 1. In Table 1, the predicted trim condition shows good agreements with those of flight test although a fuselage, hub, and blade elastic deformation effects are not considered.

Table 1. Control and flapping angles of AH-1G rotor

Blade Motion	θ_0	θ_{1s}	θ_{1c}	β_{1s}	β_{1c}
Flight Test (Ref. 15)	6.0	-5.5	1.7	-0.15	2.13
Yang et al., after trim (Ref. 17)	8.0	-6.5	2.5	-0.15	2.13
Present Prediction, after trim	6.1	-5.6	1.4	-0.15	2.13

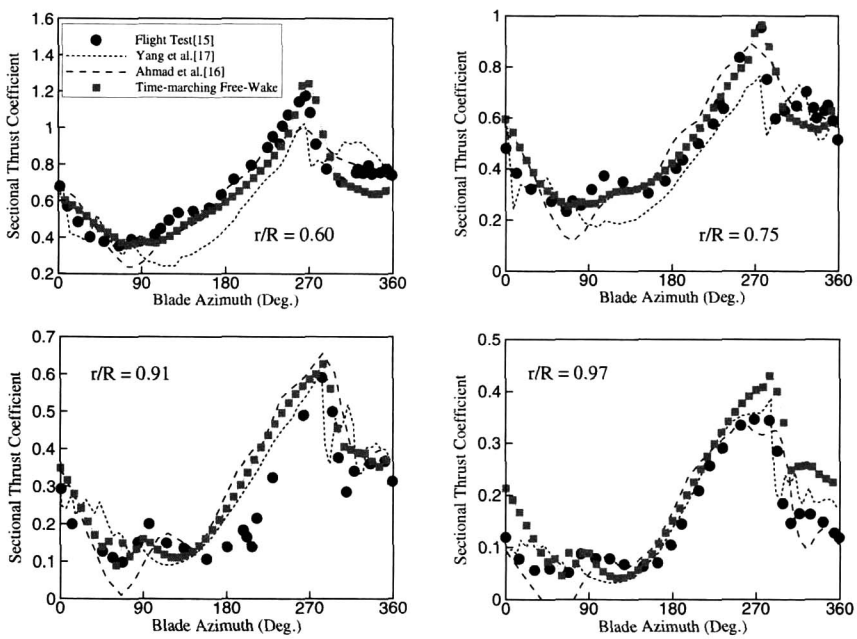

Fig. 7. Sectional thrust coefficient comparisons for AH-1G rotor

Fig. 7 compares the present computed normal load data with the measured airloads[15] and previous studies[16, 17]. The present predicted results agree very well with flight test data. Therefore, the present numerical scheme, i.e. time-marching free wake method with trim routine is working very well even in forward flight condition.

Prediction of inflow in forward flight

To validate the time averaged inflow prediction capability of the present method, the same experiment condition as Elliott et al. [18] is simulated. The experimental data were measured one chord above the rotor disk by using a laser Doppler velocimetry system. The rotor was trimmed such that the TPP(Tip Path Plane) was perpendicular to the rotor shaft, with a forward shaft tilt of -3^o. The conditions of the simulation are $C_T = 0.008, \alpha_s = -3^o$ and $\mu = 0.15$.

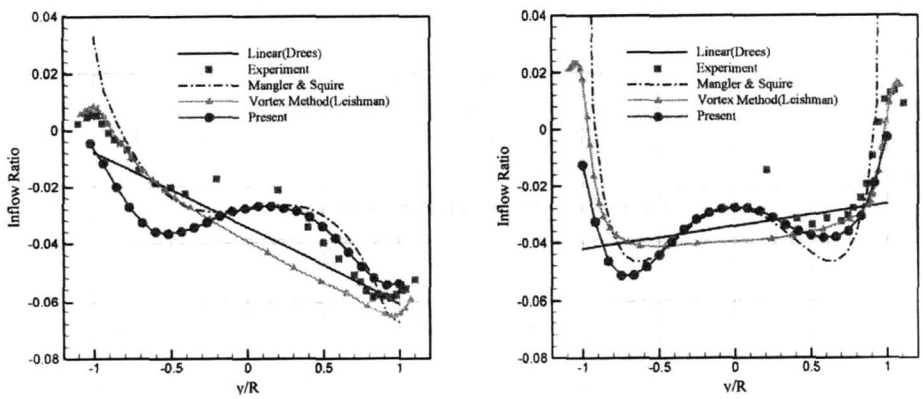

(a) Longitudinal inflow (b) Lateral inflow

Fig. 8. Comparisons of inflow ratio across the disk in forward flight ($\mu = 0.15$)

Fig. 8 shows the comparisons of inflow ratio between those of Drees linear inflow model[9], the experimental data[18], Mangler & Squire model[9], and the predicted result that is simulated by using the present scheme. In case of Mangler & Squire model, the average value of Type I and Type III is used as recommended in Ref. 9. Since the model of experiment is not employed with an isolated rotor but a rotor with fuselage, the calculated results cannot be considered in entire attributes of experimental data.

The predicted result shows reasonably good agreements with the experimental data. In Fig. 8(a), some discrepancies of longitudinal inflow near the leading edge region of the rotor disk (negative x/R in Fig. 8(a) may be caused by up-wash due to a fuselage effect. Lateral inflow is predicted with better agreement as shown in Fig. 8(b). The present results show more reasonable accuracy in inboard region(x/R < 0.8) that the other free vortex wake method[9].

Results and Discussion

Tip-vortex instability in transition flight

Tip-vortex motions of a transition flight from hover to the low advance ratio forward flight are simulated by using the time-marching free-wake method. The rotor used in this calculation is same as that used for the tip-vortex instability study of hover flight. To get a fully converged solution of hovering tip-vortex instability, the calculation is performed during 20 revolutions in

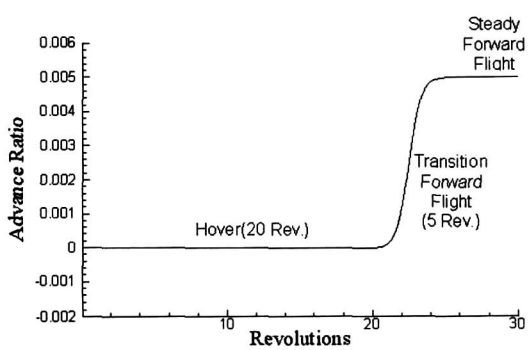

Fig. 9. Advance ratio history with respect to the rotor revolutions

hover and then starts forward flight with full wake structure as an initial condition. The final target advance ratio is set to 0.05 and is reached after five revolutions from a hover flight as shown in Fig. 9.

Twenty-four time steps per blade revolution for initial hover flight condition and for transition forward flight are taken for the present calculations. The tip vortex core radius is taken as 10% of the chord length that is commonly used in rotor wake simulations[13].

Table 2. Trim condition (μ=0.05)

Blade Motion	θ_0	θ_{1s}	θ_{1c}	β_{1s}	β_{1c}
Trim Condition (at μ=0.05)	11.5	-2.66	0.94	0.0	0.0

Table 2 shows the predicted trim condition of $C_t = 0.0066$ (same C_t with hover flight) at the advance ratio μ=0.05. It is assumed that the isolated rotor move forward with this trim

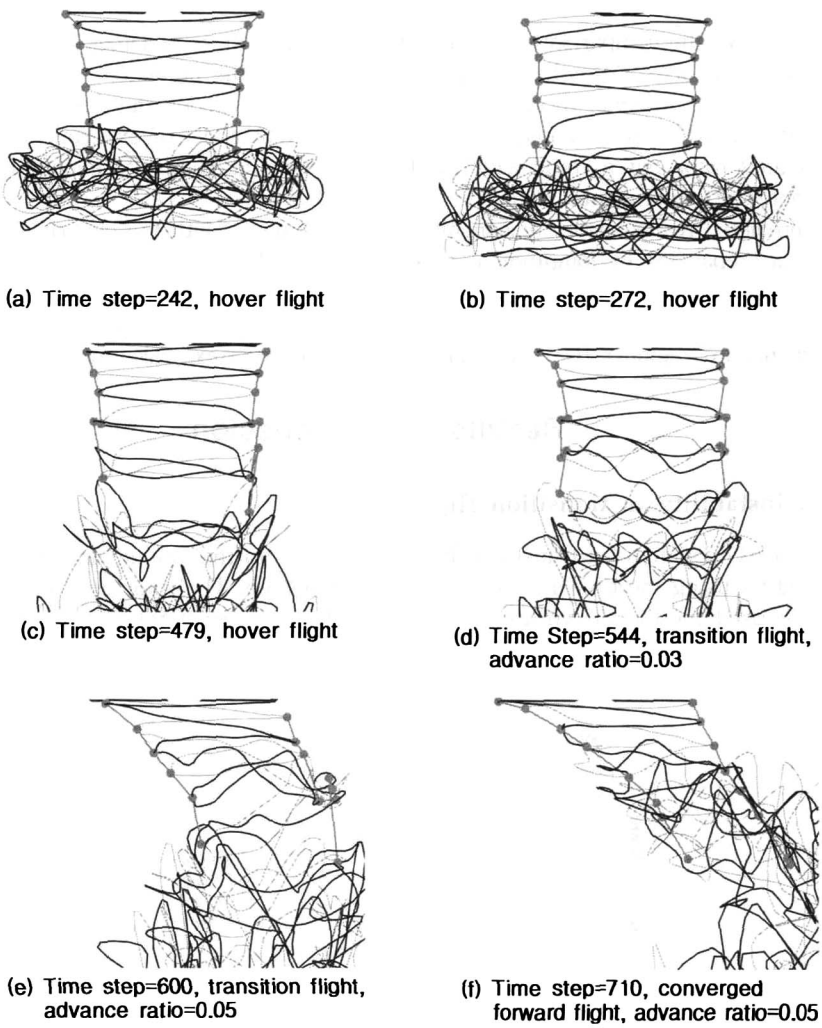

(a) Time step=242, hover flight

(b) Time step=272, hover flight

(c) Time step=479, hover flight

(d) Time Step=544, transition flight, advance ratio=0.03

(e) Time step=600, transition flight, advance ratio=0.05

(f) Time step=710, converged forward flight, advance ratio=0.05

Fig. 10. 3-D view and cross sectional view of tip vortices geometries during transition flight(final advance ratio=0.05)

condition during transient flight after 20 revolutions, i.e. time step=480. Fig. 10 shows the wake geometries at certain time steps of hover flights (Fig. 10(a)-(c)), transition forward flights (Fig. 10(d) & (e)), and a converged forward flight (Fig. 10(f)). Fig. 10(a) shows contracted fine and stable tip-vortex geometries, that is usually modeled as the traditional tip-vortex concept. Fig. 10 (b) shows typical tip-vortex structure during a vortex instability period. The pairing induced by far wake perturbation occurs from far wake region near the initial wake bundles. Then, the pairing point in hover moves toward rotor disk and converged to some position around 76% radius beneath the rotor disk as shown in Fig. 10(c).

At the instant of very slow forward flight condition (μ=0.03) during transient flight, the pairing phenomenon still can be observed as shown in Fig. 10(d). After reaching the target forward speed (μ=0.05), the vortex pairing bundles is convected to the down-stream (Fig. 10(e)) and disappears as shown in Fig. 10(f). In Fig. 10(f), the cross-sectional tip vortex trajectory shows the same as the traditional tip-vortex geometries of the forward flight.

Tip-vortex instability in steady slow forward flight

For further more investigations about tip-vortex instability at very slow forward speed, the tip-vortex geometries of a steady forward flight (μ=0.03) are calculated. To simulate the steady forward flights, it is assumed that the isolated rotor at hover initially moves forward to get the target forward speed within an one revolution. The trim condition of μ=0.03 is calculated as shown in Table 3.

Table 3. Trim condition (μ=0.03)

Blade Motion	θ_0	θ_{1s}	θ_{1c}	β_{1s}	β_{1c}
Trim Condition (at μ=0.03)	11.4	-2.15	0.46	0.0	0.0

The tip-vortex pairing occurs at the very slow steady forward flight (μ=0.03) as shown in Fig. 11. The differences between vortex pairing phenomenon in a hover and axial flight and those in this flight are that the z-direction location of pairing position(z/R=1.0) at this condition is lower than that of hover case because the free stream seems to make the pairing be convected

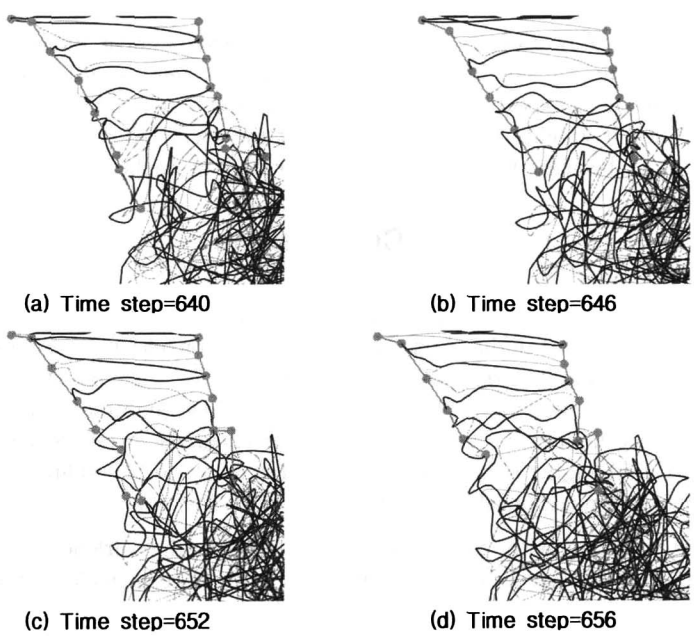

(a) Time step=640 (b) Time step=646

(c) Time step=652 (d) Time step=656

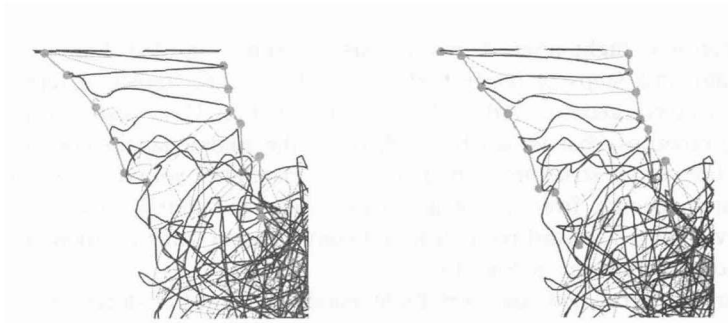

(e) Time step=660 (f) Time step=664

Fig. 11. 3-D view and cross sectional view of tip vortices geometries for the very slow steady forward flight(μ=0.03)

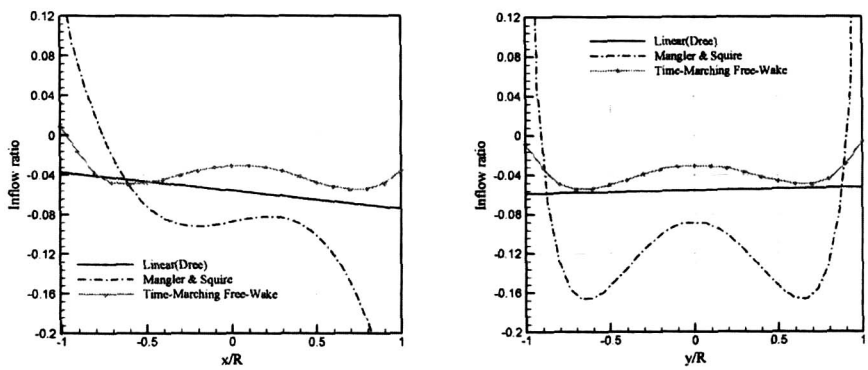

(a) Longitudinal inflow (b) Lateral Inflow

Fig. 12. Comparisons of inflow ratio across the disk in very slow forward flight(μ=0.03)

downstream. And the pairing does not occur at the front cross-sectional vortex trajectory line (left one in Fig. 11), however occurs at the rear cross-sectional vortex trajectory line (right one in Fig. 11).

The calculated inflow ratio is compared with the Drees linear model and Mangler & Squire model, as shown in Fig. 12. The latter two models are not valid in inflow calculation for very low advance ratio flight. It is expected that the inflow distribution is quite complex and unsteady due to the proximity and instability of vortices, however the predicted results show the smooth curves as shown in Fig. 12 because the time averaged concept is applied.

Conclusions

Time-marching free-wake method has been developed and validated in predicting the tip vortex instability of vertical flight. And the trim routine considering the flapping is added for the prediction of forward flight attributes. Main advantage of the robust and accurate numerical scheme is that the every details of phenomena and physical quantities can be investigated. There are still lots of uncertainties of vortex dynamics particularly in transition flight and very low advance ratio forward flight. It is necessary to simulate various conditions in this range.

The following conclusions have been drawn from this study:

1. Present scheme with trim routine can predict the airloads of forward flight very accurately, and time averaged inflow distributions with a reasonable accuracy. Fuselage model have to be employed to enhance the accuracy level.

2. By using a tip-vortex trajectory tracking method, the tip-vortex pairing process are clearly observed in transient flight(μ=0.03) and disappears at a slightly higher advance ratio(μ=0.05).

3. According to the very slow steady flight simulation at μ=0.03, it is confirmed the tip-vortex pairing process occurred in initial hover is continued in the rear part of rotor disk and not occurs in the front part. The free stream may make the instability of front part be re-stable. And the z-direction location of pairing position(z/R=1.0) at this condition is lower than that of hover case because the free stream seems to make the pairing be convected downstream. There must be the threshold advance ratio which can be found through the further calculations.

4. Time averaged inflow in μ=0.03 steady case is predicted as a smooth curve and the linear inflow model has more reasonable accuracy than Mangler & Squire model.

Acknowledgement

This study was a part of results of the project entitled "Innovative Technology Study for the Jet-Smooth Quiet Rotor System" of NRL Program.

References

1. Landgrebe, A. J., "The Wake Geometry of a Hovering Helicopter Rotor and Its Influence on Rotor Performance", *J. American Helicopter Soc.*, 17, (4), Oct., 1972, pp. 3~15.

2. Tangler, J. L., Wohlfed, R. M., and Miley, S. J., "An Experimental Investigation of Vortex Stability, Tip Shapes, Compressibility, and Noise for Hovering Model Rotor", *NASA CR-2305*, 1973.

3. Widnall, S. E., "The Stability of a Helical Vortex Filament", *Journal of Fluid Mechanics*, Vol. 54, No. 4, 1972, pp. 641-663.

4. Gupta, B. P., and Loewy, R. G., "Theoretical Analysis of the Aerodynamic Stability of Multiple, Interdigitated Helical Vortices", *AIAA Journal*, Vol. 12, No. 10, October 1974, pp. 1381~1387.

5. Martin, P. B., Bhagwat, M. J., and Leishman, J. G., "Strobed Laser-Sheet Visualization of a Helicopter Rotor Wake", Paper PF118, *Proceedings of PSFVIP-2*, Honolulu, HI, May 1999.

6. Caradonna, F., Hendley, E., Silva, M., Huang, S., Komerath, N., Reddy, U., Mahalingam, R., Funk, R., Ames R., Darden, L., Villareal, L., Gregory, and Wong, O., "An Experimental Study of a Rotor In Axial Flight", *AHS Specialists' Meeting on Aerodynamics and Aeroacoustics*, Williamsburg, VA, Oct. 1997.

7. Chung, K.H., Na, S.U., Jeon, W. and Lee, D.J., "A Study on Rotor Tip Vortex Pairing Phenomenon by Using a Time-Marchig-Free-Wake Method", *American Helicopter Society 56th Annual Forum*, Virginia Beach, May 2-4, 2000.

8. Chung, K.H. and Lee, D.J., " Numerical Prediction of Rotor Tip Vortex Roll-up in Climb Flight by Using a Time-Marchig-Free-Wake Method", *Computational Fluid Dynamics Journal*, pp. 80~88, vol. 12, no.1, April, 2003.

9. Leishman, J. G., *Principles of Helicopter Aerodynamics*, 2000, Cambridge Univ. Press, pp.115~123.

10. Lee, D. J. and Na, S. U., "Predictions of Helicopter Wake Geometry and Air Loadings by using a Time Marching Free Wake Method", *Proc. 1st Forum Russian Helicopter Soc.*, Moscow, Russia, 1994, pp. 69~85.

11. Na, S. U. and Lee, D. J., "Numerical Simulations of Wake Structure Generated by Rotating Blades Using a Time-Marching Free-Vortex-Blob Method", *European Journal of Mechanics*, 18, (1), 1999, pp. 147~159.

12. Moore, D. W., "Finite Amplitude Waves on Aircraft Trailing Vortices," *Aeronautical Quarterly*, 231972, pp. 307~314.

13. Rosenhead, L. "The Spread of Vorticity in The Wake behind a Cylinder", *Proc. Roy. Soc.*, A127, 1930, pp. 590~612.

14. Leishman, J. G., Baker, A. and Coyne, A., "Measurements of Rotor Tip vortices Using Three-Component Laser Doppler Velocimetry", *J. American Helicopter Society*, 41, (4), Oct. 1996, pp. 342~353.

15. Cross, J. L., and Watts, M. E., "Tip Aerodynamics and Acoustics Test:A Report and Data Survey", *NASA-RP-1179*, NASA Ames Research Center, Dec. 1988.

16. Ahmad, J., and Duque, E. P. N., "Helicopter Rotor Blade Computation in Unsteady Flows Using Moving Embedded Grids", AIAA Paper 94~19g22, June 1994.

17. Yang, Z., Sankar, L. N., Smith, M. J.and Bauchau O.,"Recent Improvements to a Hybrid Method for Rotors in Forward Flight", *Journal of Aircraft*, Vol. 39, No. 5, September-October, 2002.

18. Elliot, J. W., Althoff, S. L., and Sailey, R. H., "Inflow Measurements Made with a Laser Velocimeter on a Helicopter Model in Forward Flight", Vol. I, *NASA TM-100541*, 1988.